Sagittal split ramus osteotomy-related biomechanical properties

G. Rougier, J. Boisson, N. Thurieau, N. Kogane, F. Mangione, A. Picard, J. Dallard, L. Cherfa, Fabien Szmytka, N. Kadlub

Title: RAMUS SAGITTAL OSTEOTOMY RELATED BIOMECHANICAL PROPERTIES.

Authors:

Guillaume ROUGIER[1,2], Jean BOISSON[2], Nicolas THURIEAU[2], Nicolas KOGANE[1,2], Francesca MANGIONE[3], Arnaud PICARD [1,4], Jeremy DALLARD[2], Lahcene CHERFA[2], Fabien SZMYTKA[2*], Natacha KADLUB[1,4*]

*: co-last authorship

1: Department of Maxillofacial Surgery and Plastic Surgery, National Reference Center for Cleft Lip and Palate, Hôpital Universitaire Necker-Enfants Malades, Paris, France
2: IMSIA, ENSTA Paris-Tech, Department of Mechanical Engineering, Palaiseau, France
3: EA 2496 Laboratory Orofacial Pathologies, Imagery and Biotherapies, Dental School and Life imaging Platform (PIV), University Paris Descartes Sorbonne Paris Cité, Montrouge, France
4: University of Paris, Paris, France

Corresponding author:
ROUGIER.G, Department of Maxillofacial Surgery and Plastic Surgery, National Reference Center for Cleft Lip and Palate, Hôpital Universitaire Necker-Enfants Malades, Paris, France
Phone : +33619948047, email : guillaumerougier75@gmail.com

Financial disclosure : Study performed with the kind financial help of La Fondation des Gueules Cassées et la Fondation pour l'Étude et la Recherche du Corps Médical

Keywords: Ramus sagittal osteotomy; biomechanical properties; mandibular bone; cadaveric tests; surgical simulation

Word count: Entire body of text (2499), Abstract (186), Introduction (223), Material and methods (905), Results (387), Discussion (984)

Sagittal split ramus osteotomy-related biomechanical properties

Abstract

Sagittal split ramus osteotomy (SSRO) is one of the most common maxillofacial operations, and the technique relies in a directed fracture involving different biomechanical variables. The aim of this study was to find out the biomechanical characteristics involved during each step of sagittal split osteotomy. We sampled eight fully dentate human mandibles and used the right side for hardness tests and the left side for a traction-to-fracture test within an unfinished SSRO. Right sides were sampled in five parts underlying the corticotomy course and tested with a hardness testing automatic machine. The mean hardness measures ranked to 21.5 HV (Hardness Vickers Unit): 17.8 HV; 27.4 HV; 22.7 HV; 28.7 HV; for the lingual, diagonal, vestibular, full ramus, and full body samples, respectively. Left sides were cut using Epker's technique, and split with an electromechanical testing machine. The higher values reached before fracture in the traction-to-fracture tests ranked to 99.1N/6.7mm; 137.2N/10.8mm; 36.2N/4.2mm; 93.0N/7.3mm; 74.0N/8.1mm; 78.1N/4.5mm; 90.9N/10.6mm; and 64.7N/4.1mm, respectively, for specimens I, II, III, IV, V, VI, VII and VIII. This study provides to our knowledge the first biomechanical characteristics of SSRO and proposes a reproducible method for evaluation.

Keywords: Ramus sagittal osteotomy; biomechanical properties; mandibular bone; cadaveric tests; surgical simulation

Introduction

Understanding the overall structure and functioning of any material implies an understanding and documentation of its mechanical properties. When it comes to bone surgery, an understanding of the underlying mechanical properties is essential for mastery of the surgical intervention. Sagittal split osteotomy of the mandibular ramus (SSRO) is a common surgical intervention in maxillofacial surgery, which consists of creating a directed fracture along the alveolar inferior nerve canal. This requires three steps: the corticotomy, fracture of the medullary bone, and then final full fracture. One feared complication is the wrong fracture of the mandible, commonly called a "bad split", which provokes a highly unstable fracture and jeopardises the whole operation. [1, 2] As SSRO consists of a directed fracture, it is essential to understand its biomechanical aspects first. Many studies have reported the various biomechanical characteristics of the mandibular bone, [3 - 6] but none has reported the direct biomechanical variable specifically implied in each of the different surgical steps through laboratory experiments. Defining the hardness of cancellous and cortical bone and the steps needed to split the mandible are necessary to develop a further robotic tool, or 3-dimensional printed high fidelity model for training and surgery.

The aim of this study is to describe the characteristics involved in the SSRO with biomechanical testing.

Material and methods

From January to June 2019, 10 fresh human cadavers (five male and five female, numbered I -X) were dissected. (The cadavers were provided by l'École de Chirurgie du Fer à Moulin, Agence Générale des Produits de Santé-AGEPS, Assistance Publique des Hôpitaux de Paris-APHP). Permission for the study was obtained from the institutional board (Ecole de

Chirurgie, AGEPS, APHP). All cadaveric subjects had given their consent for the use of their bodies for medical research. Lengths of cold preservation in a storage room at 4°C extended from 1 - 2 days before harvest and ages at death ranged from 41 - 65 years.

Sampling (Fig. 1)

We sampled eight fully-dentate entire mandibles (specimens I to VIII) and split them in two. The left side was used for the traction-to-fracture test within an unfinished SSRO and the right side was used for the hardness tests. First "testing specimens" (specimens IX and X, data not shown) were used to develop our protocol and ensure the reproducibility of our tests and were excluded. Each right side was sampled in five parts underlying the process of the osteotomy: lingual cortical bone sample; vestibular diagonal ramus cortical bone sample; vestibular horizontal corpus cortical bone sample; full ramus piercing sandwich, with vestibular cortical, medullary and lingual cortical bone sample, tested on the lingual face; and full body piercing sandwich, with vestibular cortical, medullary, and lingual cortical bone sample, tested on the vestibular face.

The circumferential cortical bone was cut at the edge of the basilar border, to ensure that no cortical basilar bony resistance could affect our measures. Also, samples 4 and 5 have been harvested to find out whether the medullary part could have a deciding role in the strain forces applied by the burr on the cortical bone, by comparing their values with those obtained with the simple cortical samples harvested at the same location. All samples measured $1cm^2$ and were harvested with a sagittal saw.

Hardness tests

The objective of those tests was to find out the hardness of the bone under the tip of the hardness machine, simulating the surgeon's burr when it was applied to the mandible to make the corticotomy. Each sample was tested with a hardness testing automatic Fischer® machine

(Microduromètre Fischerscope HM2000, Fischer Technology Inc.750 Marshall Phelps Rd. CT 06095) calibrated with a pyramidal Vickers tip, using 6 x 6 matrices to keep 30 relevant values after deleting the three lowest and three highest values obtained in hardness Vickers Units (HV). All samples were hot press-mounted in a standard resin with a 3 minute heating time and a 2.5 minute cooling time at a 250-bar pressure, and then automatically polished under water using a polishing disc (80 grains) until a plain surface was obtained. It was cut with a sagittal saw afterwards to ensure that the depth of the mounted sample was sufficient. Each hardness measurement was made for a 2000 mN load, with an increase and decrease time of 20 seconds, and a five seconds' peak time. Each hardness measurement was checked, and the remaining tip print photographed.

Traction-to-fracture test (Figs. 2 and 3)

For all left mandibular sides, we did a SSRO according to Epker's technique[1] in three steps as follows: the corticotomy, using a Lindeman burr through the cortical surface to access the medullary bone; the split preparation, using an osteotome and a mallet with special care taken to create a passage externally to the alveolar mandibular nerve; and the final fracture. The cutting was done at a speed of $2mm.min^{-1}$ until fracture, using an automatic Instron® testing machine (Instron 5967 Instron®, Division of ITW Limited) with specific home-made bits mounted on two subperiosteal elevators and introduced inside the uncut osteotomy, and positioned facing the ramus at the depth of the Spix spine and the horizontal branch at the edge of the basilar border. We chose a slow speed so that we could see precisely every loss of load or uncomplete fracture before final fracture. We chose to do the osteotomy with a Lindemann burr to have a wide approach to the medullary bone so that the subperiosteal elevators could be introduced easily. Each half-left mandible was then cut with measurement

of the necessary force (N) depending on the displacement (l) of the two grips, and of the original gradient coefficient.

Statistical analysis

We compared the values obtained from hardness tests among the different specimens, sample per sample, and used a Z-test to compare the mean value of each sample with the whole specimen pool. We accepted that the difference was significant if the absolute value of the Z-test result was above 1.96 for α=0.05, β=0.2, bilateral test, and p value<0.05. An analysis of variance (ANOVA) was also used: with n=30 measures/sample, k=5 samples/specimen, n=150 (30*5) measures in total, based on the null hypothesis that overall distributions of those sample values were equals, we made our ANOVA calculations with $F^{k-1}_{N-k;\alpha}$ degrees of freedom, and rejected the null hypothesis if $F^0 > F^4_{145;0.05} \approx F^4_{100;0.05} = 2.46$ for each specimen. Regarding traction to fracture tests, we calculated the original gradient coefficients for each curve. All results are given as mean (SD). All results were considered significant if the p value was <0.05. All statistical analyses were made with the statistical software IBM SPSS Statistics for Windows, (version 23.0, IBM Corp).

Results

Hardness tests (Figs 1, 4, and 5, Table 1)

Our results for hardness measurements are given as mean (SD) HV units and are summarised in Fig. 1. Each hardness measure was checked and photographed to ensure the test had worked properly. We compared the hardness measures distribution for samples 1 and 4 and 3 and 5, respectively, given their close locations, to find out if the medullary bone component exerts a significant difference on hardness measures (Fig. 4*).* Mean (SD) hardness measures values ranked to 21.5 (8.1); 17.8 (8.1); 27.4 (8.6); 22.7 (10.6); and 28.7 (9.6) HV, respectively, for the lingual cortical samples, the diagonal cortical samples, the vestibular cortical samples, the full ramus samples and the full corpus samples.

There were significant differences between samples 1 and 2 (Z-test=4,61, $p<0.001$), samples 1 and 3 (Z-test=7.76, $p<0.001$), samples 1 and 5 (Z-test=9.2, $p<0.001$), samples 2 and 3 (Z-test=11.75, $p<0.001$), samples 2 and 4 (Z-test=5.38, $p<0.001$), samples 2 and 5 (Z-test=12.9, $p<0.001$), samples 3 and 4 (Z-test=5.34, $p<0.001$), samples 4 and 5 (Z-test=6.76, $p<0.001$). No significant differences were found between the means of samples 1 and 4 (Z-test: 1.41),or for samples 3 and 5 (Z-test: 1.6).**AQ: either give exact p value or omit the p value if the difference is not significant. NS is not acceptable.** Significant differences for the distribution of overall measurements between each type of sample were retrieved out of our ANOVA calculation: F-values were: 18.07 ($p<0.001$), 113.13($p<0.001$), 64.20 ($p<0.001$), 19.14($p<0.001$), 37.24 ($p<0.001$), 31.3 ($p<0.001$), 13.5 ($p<0.001$), 33.5 ($p<0.001$) for specimens I, II, III, IV, V, VI, VII, and VIII, respectively

Traction-to-fracture measurements (Fig. 5)

Our results for mean (SD) traction to fracture measurements are summarised in Fig. 5. For each curve the higher value of the *y*-axis corresponds to the necessary load to provoke the directed fracture and complete the osteotomy. The higher values reached before fracture in our traction-to-fracture tests ranked to: 99.1N/6.7mm; 137.2N/10.8mm; 36.2N/4.2mm; 93.0N/7.3mm; 74.0N/8.1mm; 78.1N/4.5mm; 90.9N/10.6mm; 64.7N/4.1mm for specimens I, II, III, IV, V, VI, VII and VIII, respectively. The original gradient coefficients were 24.1 (r^2=0.95); 14,4 (r^2=0.91); 8,3 (r^2=0.93); 9,5 (r^2=0.98); 14,3 (r^2=0.93); 20.7 (r^2=0.99); 10.8 (r^2=0.90); 14.8 (r^2=0.79); mean=14.58, SD=5.46 for specimens I, II, III, IV, V, VI, VII, and VIII. There were no "bad splits" and the mandibular nerve remained untouched on the internal valve for all our traction-to-fracture tests (Fig. 3).

Discussion

In this original study, the objective was to find out which mandibular mechanical properties were involved in direct surgical applications. Many studies have characterised the biomechanical properties of the mandibular bone over the past 30 years. As important and relevant as those studies are, none of them were used to improve surgical practice or to create biomechanically faithful replicas in 3-dimensional printing. We chose the Epker osteotomy to explore the biomechanical characteristics of the mandible for two reasons: it has been well defined and is used all over the world,[1] and it involves various types of mechanical stress, such as torsion, traction, hardness, crack propagation and, finally, fracture, which is interesting from a mechanical point of view.

Hardness of bone, a biomechanical approach for corticotomy

As far as hardness measures were concerned, we managed to design a reproducible protocol to assess the hardness of bone in a simple, precise way. All samples had significantly different mean values as long as they were from a different location: we were unable to find any significant differences between samples 1 and 4 (ramus samples) and samples 3 and 5 (vestibular horizontal branch), which seems logical given their close locations, but all other comparisons in our entire pool of samples were significant *(*Fig. 1).

The curves shown in Fig. 4 also show that the overall distribution of hardness values is similar between samples 1 and 4 on the one hand, and samples 3 and 5 on the other. As the only difference between those samples is the medullary part of the bone, this tends to emphasise that the inherent resistance to compression in part of the medullary bone may be neglected and that the cortical bone holds the major part in the resistance to the Lindemann burr during the corticotomy, for the ramus as well as the body. Such results are in accordance with other published work, including Lakatos et al [3] who reported a much lower Young's modulus value for the medullary bone of the condyle, ranging from 6.9 to 199.5 MPa, which is negligible compared with the cortical bone. Studies that have characterised the elastic properties of bone through its Young's modulus and intrinsic resistance to strains report similar results – for example, Van Eijden et al [4] (101 to 685 MPa for the ramus cortical samples) or Odin et al [5] (3GPa for the Young's modulus of circumferential cortical body samples).

Traction to fracture test, a biomechanical approach for cleavage

Traction to fracture tests rely on their simplicity and capacity to measure the stress applied between the two valves during the final fracture. The tests present different values for the maximum load reached before full fracture, ranging from 36.2 to 137.2 N for displacements ranging from 4.05 - 10.83 mm. These biases can be the result of an interspecimen variability,

which remains even if the surgical technique, protocol, and device used for each specimen are unchanged. The exact and precise course of the osteotomy can also vary from one specimen to another. However, considered the low SD of the coefficient gradient in our tests, its reproducibility can be ensured. All curves adopted a similar shape, except for specimens 6 and 8, showing multiples short load drops matching fracture propagation before cutting, and a total loss of load afterwards.

We adopted a surgical approach with a Lindemann burr to do the corticotomy, rather than a reciprocating saw, and therefore spared less cortical bone at the edge of the basilar border with a wider notch. This could have influenced our results as the risk of a bad split may be limited with a wider cut. A certain limitation to the generalisation of those results (apart from their cadaveric nature) could also be linked to the motionless position of the subperiosteal elevators inside the osteotomy during the traction to fracture test, as those are usually repositioned during the split in conventional surgery. However, such modifications could not have been made without compromising the entire interpretation of the test, which was our top priority, and in our entire group of specimens there was no bad split, and the alveolar inferior nerve always remained untouched on the external side of the internal valve, which increased its surgical interest.

We divided the major steps of Epker's osteotomy in two, and followed a protocol that we think may help many surgical teams in their approach to mechanical testing of the mandible. This original study has several strengths: first, it is the first one to our knowledge that aimed to work out the inherent biomechanical properties that are at work in the SSRO through hardness measurements and traction to fracture tests with mounted elevators. Secondly, we designed a reproducible protocol with simple variables and obtained coherent results with both biomechanical and anatomical explanations.

However, some limitations had to be overcome: we made no direct measurements of the surrounding soft tissues such as periosteum, muscles, or mucosa, and that should be done in the future to find out if 3-dimensional printed materials may match such tissues. Debelmas et al[7] have already experimented on, and reported, the measure of the stress-strain applied to the periosteum during mandibular distraction, and such experiments should be conducted on all oral, mandibular, and cervical soft tissues. Next, to complete our protocol, a study of "crack-fracture-propagation" should be made on the medullary bone. Finally, to characterise the biomechanical variables implied in the mandibular SSRO, one should keep in mind that each step of the whole operation responds to specific mechanical variables that first need to be assessed separately. Those data will help the oral and maxillofacial surgical community to create high-fidelity, 3-dimensional, printed mandibular replicas for surgical simulation by choosing appropriate materials, and overall constitute the necessary information for the making of robotic tools or mechanical accessories in orthognathic surgery.

Acknowledgements

We thank L'École de Chirurgie du Fer à Moulin, de l'AP-HP, its scientific director and headmaster Pr Pascal Frileux, his associate Djamel Taleb and all the staff, as they kindly supported all anatomical experiments inside the school.

We also thank la Fondation des Gueules Cassées and la Fondation pour l'étude et la recherche du corps médical, as they supported this original study financially.

All authors agree with the submission. This work has not been published or submitted for publication elsewhere, either completely or in part, or in another form or language.

Conflict of Interest

We have no conflicts of interest.

Ethics statement/confirmation of patients' permission

Permission to make cadaveric studies on fresh specimens was obtained from the institutional review board (Ecole de Chirurgie, AGEPS, APHP). All the cadaveric subjects had given their consent for the use of their body for medical research

QUERIES TO AUTHOR

Throughout: the journal is published in British English so any American phraseology or spelling has been corrected.

Page 6: either give exact p value or omit the p value if the difference is not significant. NS is not acceptable.

References

1. Böckmann R, Meyns J, Dik E, et al. The modifications of the sagittal ramus split osteotomy: a literature review. *Plast Reconst Surg Glob Open* 2015: **2**: e271.

2. Al-Nawas B, Kämmerer P.W, Hoffmann C, et al. Influence of osteotomy procedure and surgical experience on early complications after orthognathic surgery in the mandible. *J Craniomaxillofac Surg* 2014: **42**: e284-8.

3. Lakatos E, Lóránt M, Bojtár I. Material properties of the mandibular trabecular bone. *J Med Eng* 2014: **2014**: 470539.

4: van Eijden TM, van der Helm P, van Ruijven LJ, et al. Structural and mechanical properties of mandibular condylar bone. *J Dent Res* 2006; **85**: 33-7.

5. Odin G, Savoldelli C, Bouchard PO, et al. Determination of Young's modulus of mandibular bone using inverse analysis. *Med Eng Phys* 2010: **32**:630-7.

6. Cunha, G, Oliveira MR, Salmen FS, et al. How does bone thickness affect the split pattern of sagittal ramus osteotomy? *Int J Oral Maxillofac Surg* 2020; **49**:218-23.

7. Debelmas A, Picard A, Kadlub N, et al. Contribution of the periosteum to mandibular distraction. *PloS One* 2018: **13**: e0199116.

Legends to Figures

Figure 1. Hardness: results and sampling.

Figure 2. Traction to fracture testing. The cutting was done at 2 mm/min^{-1} until fracture, using an automatic Instron® electromagnetic testing machine showing the position of the specimen during the traction-to-fracture test.

Figure 3. Final aspect after cutting: the inferior alveolar nerve canal remains untouched.

Figure 4. Distribution of hardness measures: the x axis matches the ranking of each measure after classification from lowest to highest, and the y axis matches the hardness Vickers Unit (HV) for the entire pool of mandibles (I-VIII). Samples 1 and 4, and 3 and 5, respectively have a close distribution, as sample 2 measures the lowest values.

Figure 5. The x axis matches the displacement (mm) and the y axis matches the load applied (N). Specimens I, II, III, IV, V, and VII adopt similar curves despite the differences in

maximum load obtained before reaching full cleavage. Specimen II shows multiples of load losses matching fracture propagation (red arrows) that happen before rapid loss of load when reaching full cleavage (double-spotted orange arrow) as specimen VII. Specimen VI adopts a different gradient with a progressive loss of load after a higher value had been reached, downwards from 78.15 N to 60.54 N, then a rapid loss before reaching full fracture. Specimen VIII shows no major, rapid loss after reaching full fracture at 64.75 N. On the contrary, there was a rapid peak in the gain of load applied before fracture, followed by a progressive loss of load.

Figures

Figure 1: Hardness Results and sampling

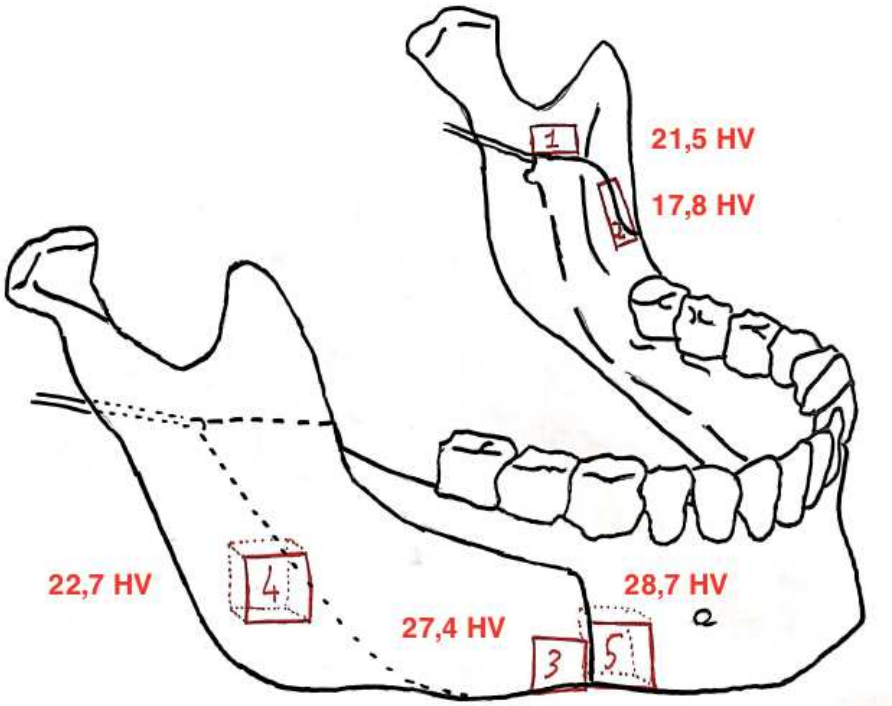

Figure 2: Traction-to-fracture testing

The cleavage was performed at a 2mm.min-1 rate until fracture, using an automatic Instron® electro-mechanical testing machine. Upper view, specimen position during the traction-to-fracture test

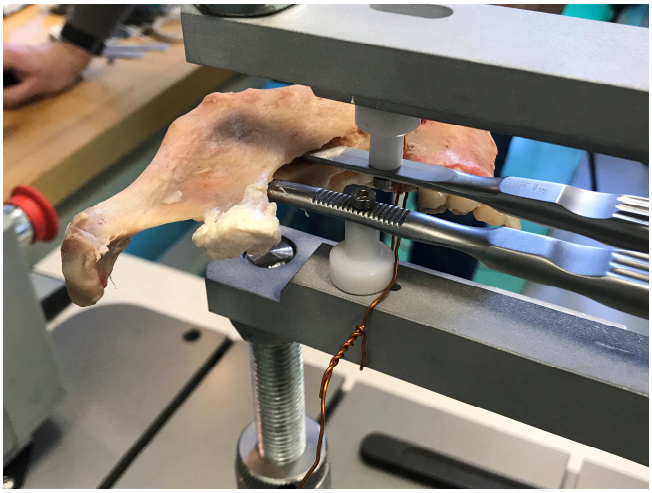

Figure 3: Completed cleavage

Final aspect after cleavage, please note that the alveolar inferior nerve canal remains untouched.

Figure 4: Hardness measures

Hardness measures distribution: The x axis matches the ranking of each measure after classification from lowest to highest, and the y axis matches the hardness Vickers measures (HV) for the entire pool of mandibles (I to VIII). Please note that samples 1 and 4 and 3 and 5 respectively, have a very close distribution as sample 2 measures show the lowest values.

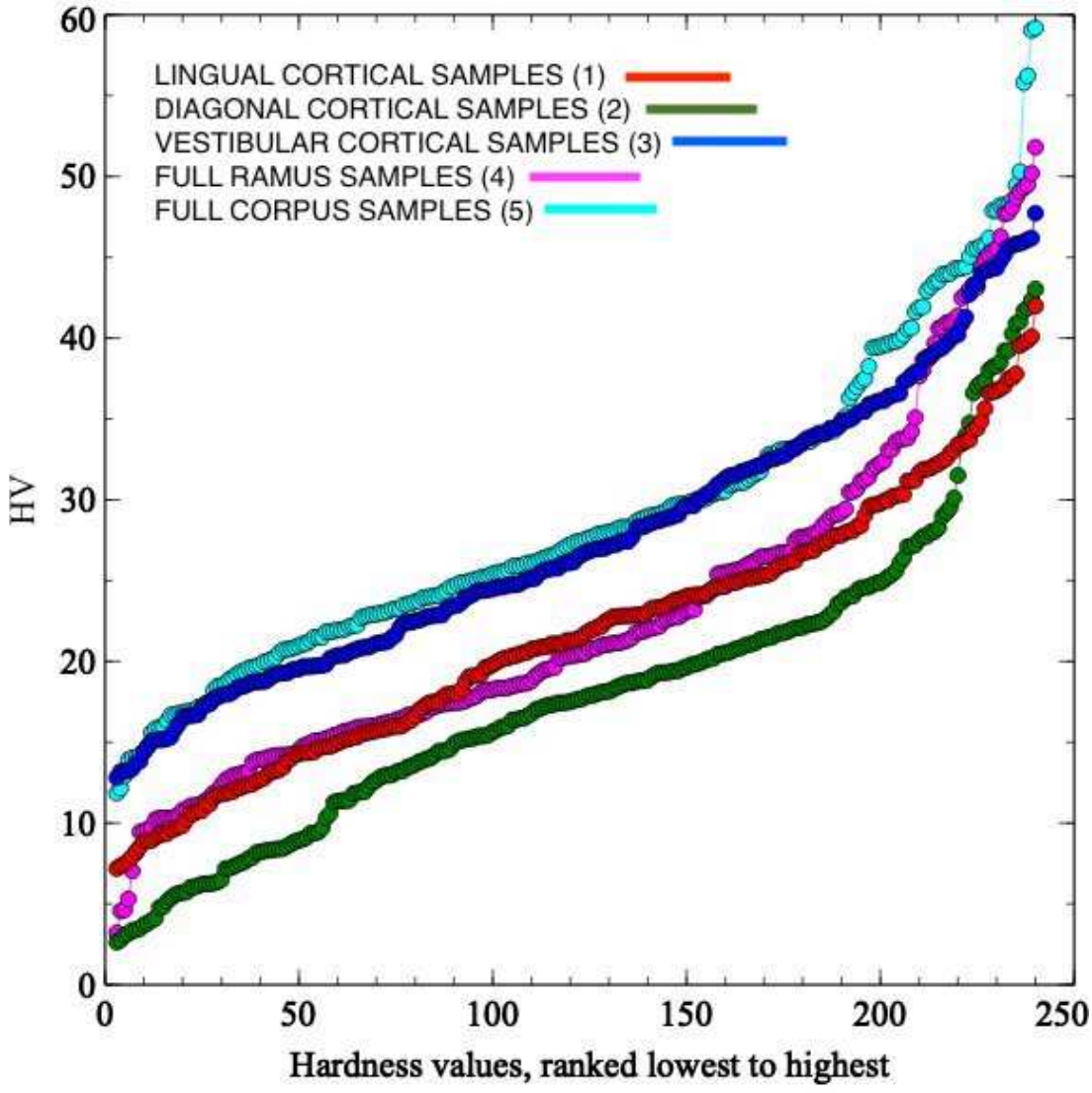

Figure 5: Traction to fracture tests results

The x axis matches the displacement (mm) and y axis matching load applied (N).

Please note that specimens I, II, III, IV, V and VII adopt a very similar curve, despite great differences in maximum load obtained before reaching full cleavage.

Specimen II shows multiples load losses matching fracture propagation (marked with red arrows) happen before rapid loss of load when reaching full cleavage (double-spotted orange arrow), as specimen VII.

Specimen VI adopt a different gradient with a progressive loss of load after the higher reached value, downward from 78,15N to 60,54 N before a rapid loss of load before reaching full cleavage.

Specimen VIII shows no major and rapid loss of load after reaching full cleavage, which happened at 64,75N. On the contrary, we observe a rapid peak in the gain of load applied before cleavage, followed by a very progressive loss of load.

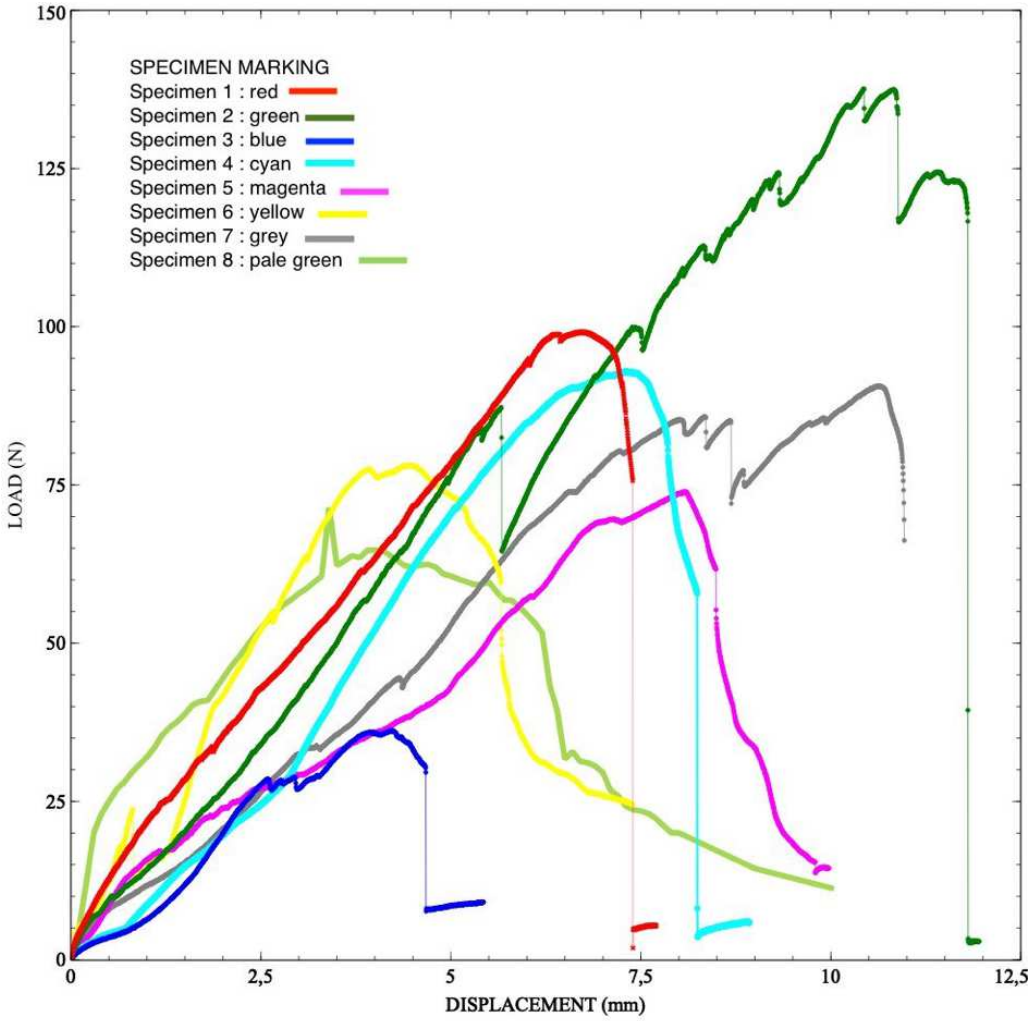
SPECIMEN MARKING
Specimen 1 : red
Specimen 2 : green
Specimen 3 : blue
Specimen 4 : cyan
Specimen 5 : magenta
Specimen 6 : yellow
Specimen 7 : grey
Specimen 8 : pale green
LOAD (N)
DISPLACEMENT (mm)
0
25
50
75
100
125
150
0
2,5
5
7,5
10
12,5

Ees 790 (19) Table edited

Table 1.

Mean (SD) Hardness Vickers (HV) measures of entire mandibles.

Specimens	Samples				
	1	2	3	4	5
I	21.06 (4.07)	23.03 (3.86)	31.26 (6.91)	24.23 (4.15)	27.63 (6.21)
II	21.61 (6.35)	5.98 (3.15)	22.70 (4.57)	16.51 (3.95)	31.32 (5.28)
III	10.93 (3.07)	9.99 (2.53)	20.20 (5.91)	15.46 (6.86)	26.97 (4.20)
IV	21.25 (2.45)	18.48 (3.41)	30.40 (6.25)	16.41 (2.77)	22.45 (4.99)
V	23.05 (4.18)	20.30 (4.43)	24.30 (3.90)	12.79 (2.65)	23.35 (5.43)
VI	12.84 (2.55)	16.32 (1.79)	20.06 (2.66)	26.09 (6.64)	20.75 (5.78)
VII	26.32 (5.58)	16.73 (11.00)	31.12 (9.71)	25.81 (5.75)	33.00 (12.81)
VIII	34.57 (3.91)	31.56 (8.56)	39.08 (5.93)	44.11 (4.17)	44.37 (3.28)
Mean (SD)	21.45 (8.09)	17.80 (9.23)	27.39 (8.65)	22.68 (10.59)	28.73 (9.65)